Fine structure of gametocytes in five species of *Haemoproteus* (Haemosporidia) from geckos and agamid lizards

Ilan PAPERNA
Department of Animal Sciences,
Faculty of Agriculture of the Hebrew University of Jerusalem,
Rehovot 76100 (Israel)
paperna@agri.huji.ac.il

Yves BOULARD
Laboratoire de Biologie Parasitaire, Protistologie, Helminthologie, EP CNRS 1790,
Muséum national d'Histoire naturelle,
61 rue Buffon, F-75231 Paris cedex 05 (France)
boulard@mnhn.fr

Paperna I. & Boulard Y. — Fine structure of gametocytes in five species of *Haemoproteus* (Haemosporidia) from geckos and agamid lizards. *Zoosystema* 22 (3) : 443-457.

ABSTRACT
The fine structure of gametocytes of five species of *Haemoproteus* from reptilian hosts was compared. The species were: *H. edomensis* from *Agama stellio*, collected East of Jerusalem; *H. mackerrasi* from *Heteronotia binoei* and *H. oedurae* from *Oedura castelnaui*, both from Northeast Australia; *H. ptyodactyli* from *Ptyodactylus hasselquistii* from the Jordan valley, and *H. tarentolae* from *Tarentola mauritanica* of Southwest France. All gametocytes showed close conformity with the previously studied reptilian and avian species of *Haemoproteus* as well as with the several known species of *Plasmodium* of reptiles and birds, in their being bound by a three-layered limiting membrane system, and in their cytoplasmic organization. At the same time, each species showed distinguishable characteristic configurations: a trapezoid organelle in *H. edomensis,* a large electron-lucent central space in *H. tarentolae* and, unlike the previous studied species, osmiophilic bodies were found: small and elongated in *H. oedurae*, very small and round in *H. ptyodactyli*, large and round in *H. tarentolae*. The presumed microgametocytes of these last three species exhibited also a lobated nucleus.

KEY WORDS
Haemoproteus,
Agama,
gecko,
lizard,
electron microscopy,
gametocytes.

RÉSUMÉ

*Ultrastructure des gamétocytes de cinq espèces d'*Haemoproteus, *hémosporidie de gecko et d'agames.*

L'ultrastructure des gamétocytes de cinq espèces d'*Haemoproteus* de Reptiles est comparée. Ces espèces sont : *H. edomensis* parasite d'*Agama stellio*, capturé à l'Est de Jérusalem ; *H. mackerrasi* chez *Heteronotia binoei* et *H. oedurae* chez *Oedura castelnaui*, ces deux hôtes venant du Nord-Est de l'Australie ; *H. ptyodactyli* chez *Ptyodactylus hasselquistii* de la vallée du Jourdain et *H. tarentolae* chez *Tarentola mauritanica* du Sud-Ouest de la France. Par leurs organites cytoplasmiques et la présence d'une enveloppe tri-membranaire, tous les gamétocytes présentent une organisation proche de celle déjà décrite chez les *Haemoproteus* et plusieurs *Plasmodium* de Reptiles et d'Oiseaux. En même temps, chaque espèce présente des structures caractéristiques : un corps trapézoïde chez *H. edomensis* ; un espace central transparent aux électrons chez *H. tarentolae* et, à la différence des espèces déjà décrites, de nombreux corps osmiophiles : petits et allongés chez *H. oedurae,* très petits et ronds chez *H. ptyodactyli,* grands et ronds chez *H. tarentolae*. Chez ces trois dernières espèces, un noyau lobé est présent dans les présumés microgamétocytes.

MOTS CLÉS
Haemoproteus,
Agames,
gecko,
lézard,
microscopie électronique,
gamétocytes.

INTRODUCTION

Haemoproteus metchnikovi infecting the turtle *Chrysemys picta* is the only species of this genus from a reptilian host where blood stages have been described at the fine structure level (Sterling 1972). Electron microscopic data are available on blood stage of two species of avian-host *Haemoproteus* (*H. columbae* Bradbury & Trager, 1968; Bradbury & Roberts 1970; Sterling & Aikawa 1973; Gallucci 1974 and *H.* (= *Parahemoproteus*) *velans* Desser, 1972). Data on the fine structure of haemosporidians from reptilian hosts also include accounts on *Plasmodium mexicanum* (Aikawa & Jordan 1968; Aikawa *et al.* 1969; Moore & Sinden 1974) and *P. tropiduri* (Scorza, 1974) and the allied genera *Garnia* and *Fallisia* (Boulard *et al.* 1987; Paperna & Boulard 1990). Recovery of *Haemoproteus* infections in *Agama stellio* and several species of geckoes (Paperna & Landau 1991) provided us with suitable material for ultrastructural studies of additional reptilian species.

MATERIAL AND METHODS

The following species were available for ultrastructural study: from the agamid *Agama stellio* Hasselquist & Linné, 1757: *Haemoproteus edomensis* Paperna & Landau, 1991 (n° 146 EB), from East of Jerusalem, Cisjordan, and from the following geckos: from *Heteronotia binoei* Gray, 1845, Townsville, North Queensland, *Haemoproteus mackerrasi* Paperna & Landau, 1991 (n° 145 EB); from *Oedura castelnaui* (Thominot, 1889), Townsville, North Queensland, *Haemoproteus oedurae* Paperna & Landau, 1991 (n° 153 EB); from *Ptyodactylus hasselquistii* (Dunndorf, 1789), Central Jordan Valley, Cisjordan, *Haemoproteus ptyodactyli* Paperna & Landau, 1991 (n° 151 EB) and from *Tarentola mauritanica* (L.), Banyuls-sur-Mer, Southwest France, *Haemoproteus tarentolae* Paperna & Landau, 1991 (n° 147 EB). Type specimens of all these species are deposited in the MNHN Paris, and stored respectively under the numero written in brackets.

Infection in the lizards was verified through blood examination. Smears were prepared from blood obtained by clipping the tip of the lizard's toe or tail. Prepared smears were air-dried and stained, after fixation in absolute methanol, in Giemsa (1/10 diluted in phosphate buffer pH 7.4) for 1 h.

For transmission electron microscopy (TEM), drawn blood collected in a non-heparinized hematocrit capillary was allowed to clot and then extracted into fixative. Where infected lizards were sacrificed, blood was withdrawn from the heart and segments of heavily vascularized organs (lungs, spleen, mesentries) were also fixed. Samples were fixed in 2.5% glutaraldehyde in 0.1 M cacodylate buffer (pH 7.4) for 24 h at 4 °C, repeatedly rinsed, post fixed in 1% osmium tetroxide in the same buffer for 1 h, and rinsed. When larger blood samples (≈ 0.5 ml) were obtainable, fixation and rinsing were carried out through repeated centrifugation (4 000 rpm) and eventual sedimentation, by centrifugation over the surface of a Nobel agar (1.3% in distilled water) layer. Further processing proceeded with segments of blood soaked agar. After dehydration in graded ethanols, material was embedded in either Epon 812 alone or mixed with Araldite. Thin sections were cut on a Reichert "Ultracut" with a diamond knife, stained on grid with uranyl acetate and lead citrate and examined in either a Jeol 100CX TEM, in the faculty of Agriculture, Israel, or a Philips EM 201, at the Centre interuniversitaire de Microscopie électronique, CIME Jussieu, Paris VI-VII, France.

OBSERVATIONS

General configuration of the intraerythrocytic stage

Ultrathin sections of the lizards' erythrocytes contained a variety of stages, from juvenile gametocytes to fully differentiated micro- and macrogametocytes. Gametocytes, the fully differentiated stages in particular, of the different studied species could be distinguished from one another, to variable degrees, by their general look (Table 1), and the texture of their cytoplasm. However, some of the species-specific patterns may be attributable to variations in the fixation and processing conditions (*H. oedurae* in particular). Within the erythrocyte, fully differentiated *H. edomensis*, *H. oedurae* and *H. ptyodactyli* retained their elongated shape (Figs 1A, B; 3C; 4A, B; 5A) and only exceptionally formed folds (Fig. 5C) or distal tail-like endings (Fig. 1C). Gametocytes of *H. mackerrasi* were usually folded within the erythrocyte (Fig. 2E, F), while those of *H. tarentolae* formed narrow or tail-like outgrowths ("tails") (Figs 6B, C, E; 7); some young gametocytes of this latter species were comprised of several interconnected segments (Fig. 6G).

Ribosomal density differences between macrogametocytes and microgametocytes were sometimes very distinct (Fig. 5E), at other times equivocal. Only some of the macrogametocytes, recognizable by their compact, small nucleus (Figs 1B, F; 6A) also demonstrated densely packed fine ribosomal contents (Figs 1A, B, F; 4B); others had a distinctly dilute or medium-dense cytoplasm (Figs 1C; 6A). What appeared to be premature gametocytes also exhibited dilute ribosomal contents (Figs 1I; 2B; 4C, D; 5B). The presumed microgametocytes with a scattered (lobate) nucleus, most conspicuously those of *H. oedurae,* also exhibited a diluted cytoplasm (Figs 3C; 4A). In the presumed microgametocytes, with lobate nucleus, of *H. ptyodactyli* (Fig. 5C-E) and *H. tarentolae* (Figs 6C, D; 7A; 8B), ribosomal density of the cytoplasm was moderate rather than low. The configuration of the nucleus was uncertain in *H. mackerrasi* due to processing damage (Figs 2E; 3A). Such processing faults could have induced further variations in the cytoplasmic consistencies, with some species being potentially more susceptible to processing treatment than others (see for example *H. oedurae*, Figs 3C; 4A). Gametocytes of *H. mackerrasi* recovered in ultrathin sections prepared from the liver, infecting proerythrocytes (Fig. 3B), and recovered from the guts of engorged mosquitoes *Culex fatigans* (Fig. 2F), did not differ from the ones found in circulating erythrocytes.

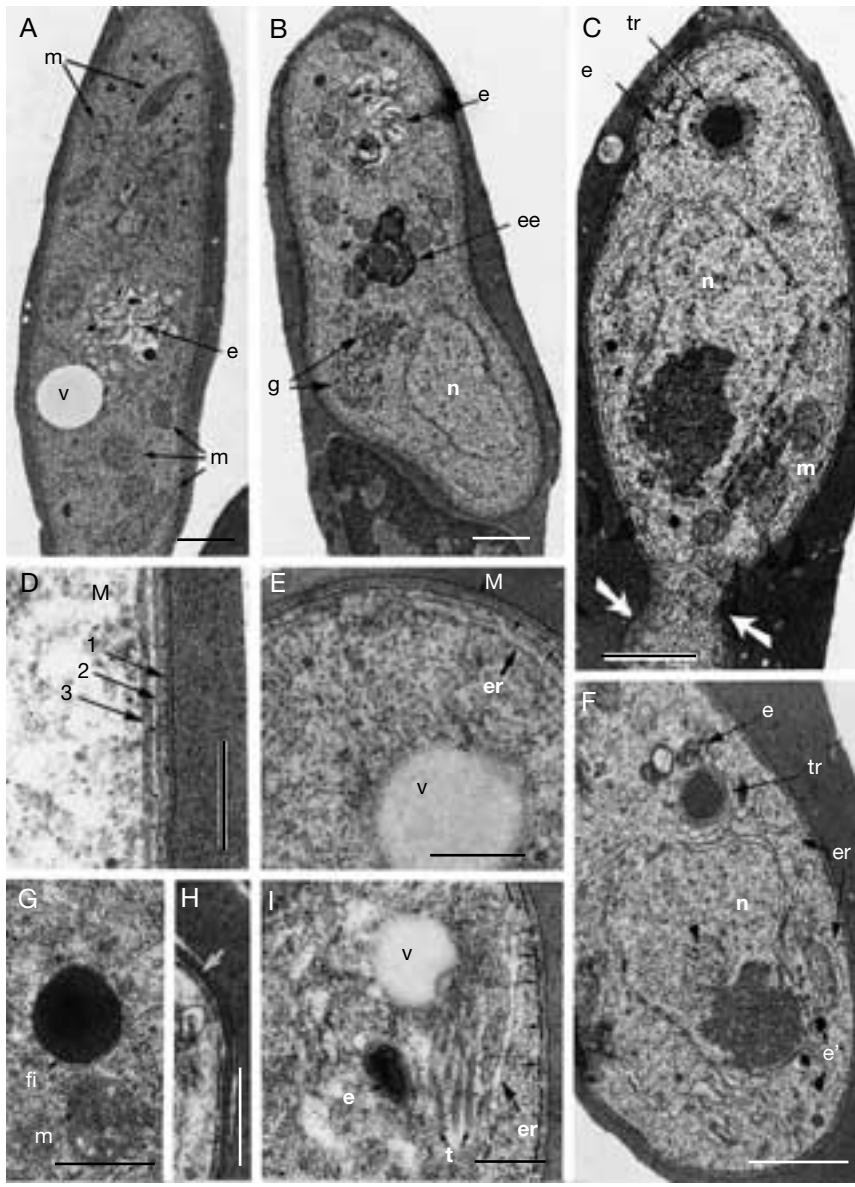

FIG. 1. — *Haemoproteus edomensis* in erythrocytes of *Agama stellio*; **A**, macrogametocyte with dense ribosomal contents, showing large inclusion with phagosomal residues, mitochondria and a vacuole; **B**, macrogametocyte (with dense ribosomal contents) showing the compact nucleus, two adjacent golgi-like tubular structures, inclusions, one containing membranous vesicular residue (e) and the other electron dense deposit (ee); **C**, macrogametocyte with tail-like ending (arrows), containing a compact nucleus with large nucleolus, an inclusion with phagosomal residue, mitochondria and "trapezoid" organelle; **D**, higher magnification view for details of the boundary membranes; **E**, detailed view of boundary membrane accompanied beneath by er extension; **F**, higher magnified view of a macrogametocyte, with compact nucleus, containing a conspicuous nucleolus, next to which can be seen an aggregate of granular matrix (arrow head); the cytoplasm contains bundles of er, a "trapezoid" and residue inclusions; **G**, unit membrane-bound food vacuole; **H**, detail from a juvenile gametocyte, showing a slit between the two lamellae of M1 and a heavy deposit between M1 and M2 (arrow); **I**, juvenile gametocyte showing a bundle of tubular structures (within a cisterna) and an electron-dense M3 membrane. Abbreviations: **e**, vacuole with phagosomal residues; **ee**, inclusion with electron-dense deposit; **e'**, inclusion filled with electron-dense material; **er**, endoplasmic reticulum and connected cisternae; **fi**, food vacuole; **g**, Golgi; M1, 2 and 3 parasite's outer, median and inner boundary membranes; **m**, mitochondria; **n**, nucleus; **t**, tubular structures; **tr**, "trapezoid organelle"; **v**, vacuole. Scale bars: A-C, F-H, 1 µm; D, 2.5 µm; E, I, 0.5 µm.

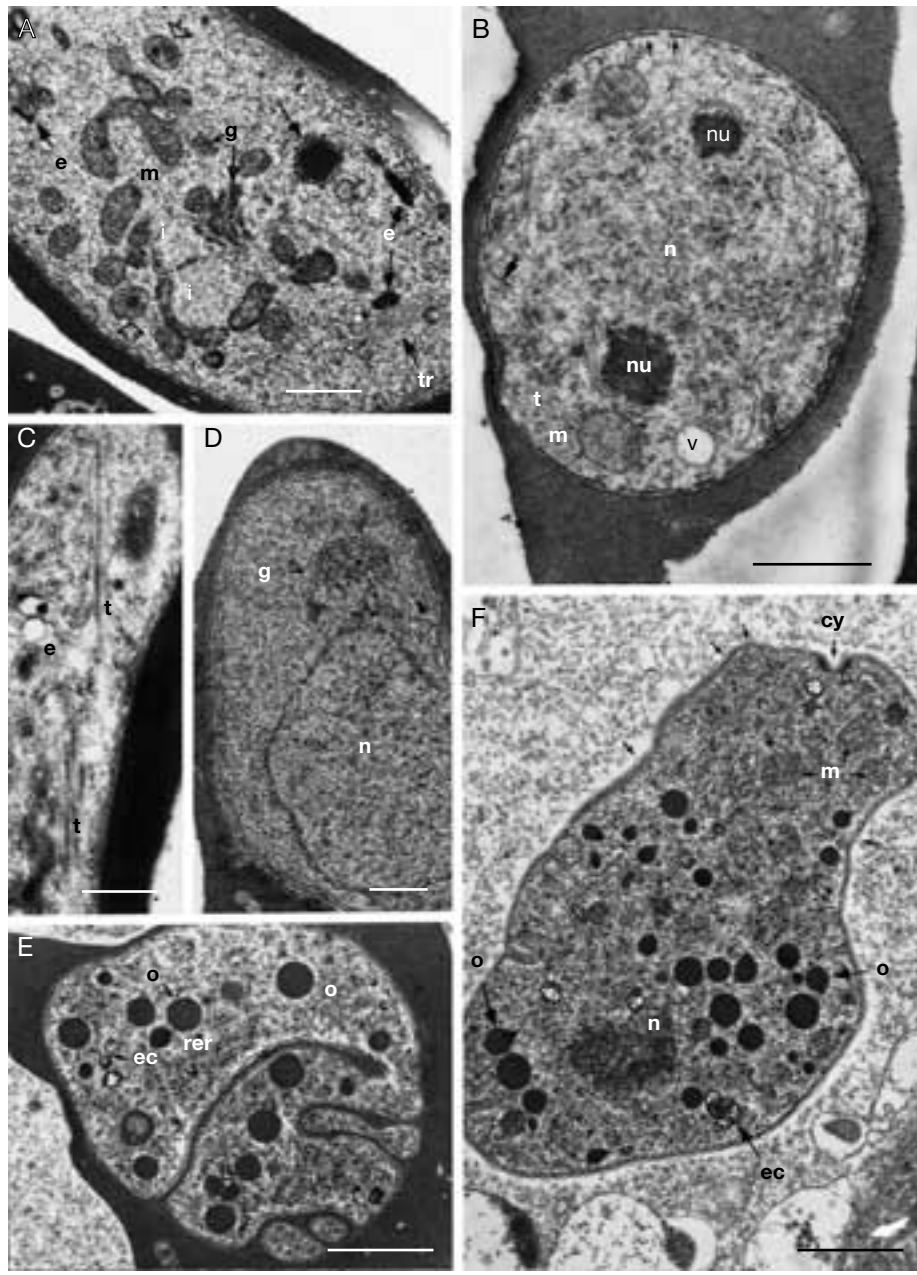

FIG. 2. — *H. edomensis* (cont.); **A**, enlarged view (macrogametocyte?) showing mitochondria, some with electron-dense deposit (open arrow), Golgi-like organelle, vacuoles with phagosomal residue, trapezoid body and inclusions of unknown nature; **B**, apparently juvenile stage with nucleus containing two (split) nucleoli, some endoplasmic reticulum is filled with electron-dense material (larger arrow), and M3 is also visible (smaller arrows), tubular structures are enclosed within an endoplasmic reticulum cisterna; **C**, view of tubulies inside cisternae; **D**, macrogametocyte with dense ribosomal contents, a compact nucleus and a Golgi-like organelle; **E-F**, *Haemoproteus mackerrasi*; **E**, *H. mackerrasi* gametocyte inside an erythrocyte of *Heteronota binoei*; **F**, *H. mackerrasi* in gut contents of *Culex fatigans* induced to engorge *Heteronota binoei*. Note loose, undulating lamina remaining of M1 membrane (arrows). Abbreviations: **cy**, cytostome; **e**, vacuole with phagosomal residues; **ec**, inclusion with crystalline deposit (hemozoin); **g**, Golgi; **m**, mitochondria; **n**, nucleus; **nu**, nucleolus; **o**, osmiophilic bodies; **rer**, rough endoplasmic reticulum; **t**, tubular structures; **tr**, "trapezoid organelle"; **v**, vacuole. Scale bars: 1 µm.

Wall membranes

All juveniles and fully differentiated gametocytes were bound by a three layered wall: layers were designated as M1 (the outermost), M2 (the middle) and M3 (the innermost) (Figs 1D, E; 3B; 4D, E). Variation in wall (pellicle) configuration was mostly intra rather than interspecific, often linked with differentiation stage.Variations were of type – unit membrane or lamina, number of laminae and their relative thicknesses – as well as in the width of the inter-membranal space and the density of the filling matrix. M1, the parasitophorous vacuole membrane consistently possessed a unit membrane structure, was usually closely tied with M2, exceptionally seen detached, apparently due to procession damage (Fig.1H). The plasma-membrane of the free macrogametocyte of *H. mackerrasi* in the mosquito's gut was disaggregating sometimes becoming reduced into a single undulating lamella (Fig. 2F). The M2 was at times very delicate (Figs 1I; 2B), or reduced to one lamina (Fig. 2B). The M2 could also become as thick as M1 (Fig. 4D, E), or even considerably thicker (Fig. 1H).

The space between M1 and M2 was either conspicuously electron lucent (Fig. 4D, E), or variably dense (Figs 1D, H; 3A, B; 5A, D and in most *H. tarentolae*, Fig. 6). The space between M2 and M3 was always electron-lucent. M3, the inner pellicular membrane appears to be composed of two unit membranes in apposition was often distinctly thick, sometimes with electron dense deposits (Figs 1F, I; 2B; 4E in juvenile *H. edomensis* and *H. ptyodactyli*). In one instance (Fig. 4E) this membrane layer was seen to be reforming.

Cytostome and food vacuoles

Large cytostomes connected to a vacuole of electron-dense contents, the presumed pinched-off erythrocyte segment, were seen only in one juvenile gametocyte of *H. ptyodactyli* (Fig. 5B). A cytostome, without accompanying vacuole, was seen in *H. mackerrasi* macrogametocytes (Fig. 2F). In addition a vacuole with homogeneous electron-dense contents, seen in *H. edomensis* (Fig. 1G) and *H. tarentolae* (Fig. 8A), seemed to be a food vacuole formed by the cytostome. Both this and the vacuole – still connected to the cytostome – were enclosed in two unit membranes. Digest residues and hemozoin accumulated in separate vacuoles: these appeared as diverse crystalloid (Figs 3A; 4B; 5E), globular (Figs 1D, I; 5B), multilaminate (Figs 1F; 4E) or other type structures (Figs 1A, B; 5A; 8A) as well as nearly homogeneous large electron dense aggregates (Fig. 1B) or small globules (Fig. 1A).

Other vacuoles and inclusions

Spherical (lipid extracted) vacuoles were found occasionally in both fully grown (Fig. 1A) and juvenile gametocytes (Figs 1E, I; 5B). Smaller vacuole, like structures or cisternae with winding borders, were also seen (Fig. 5A). There were a few inclusions with variable contents (Figs 2A; 5D). The most conspicuous, yet of undefined structure and of uncertain function, was the centrally positioned large electron-lucent (finely granular) space seen in microgametocytes of *H. tarentolae* (Figs 7A; 8B).

Tubules

Sub-pellicular microtubules were conspicuous in juvenile *H. ptyodactyli* (Fig. 4C, D), and were also sometimes traced in grown specimens (Fig. 5A). In *H. oedomensis*, longitudinal and cross section of bundles of tubular structures were founded lodged inside endoplasmic reticulum (er) cisternae (Figs 1I; 2B, C).

Endoplasmic reticulum

Endoplasmic reticulum formed an extensive network which was most conspicuously detectable in juvenile gametocytes (Figs 1F; 2B; 4E; 5B), while often being obliterated in grown stages. It also formed sub-pellicular tubular or cisternal extensions (Figs 1F, I; 6A), as well as small tubular aggregates (Fig. 2A). *H. oedurae* cytoplasm contained numerous cisternae and seemingly fragmented endoplasmic reticulum elements which may have been caused by processing aberrations (Figs 3C, D; 4A).

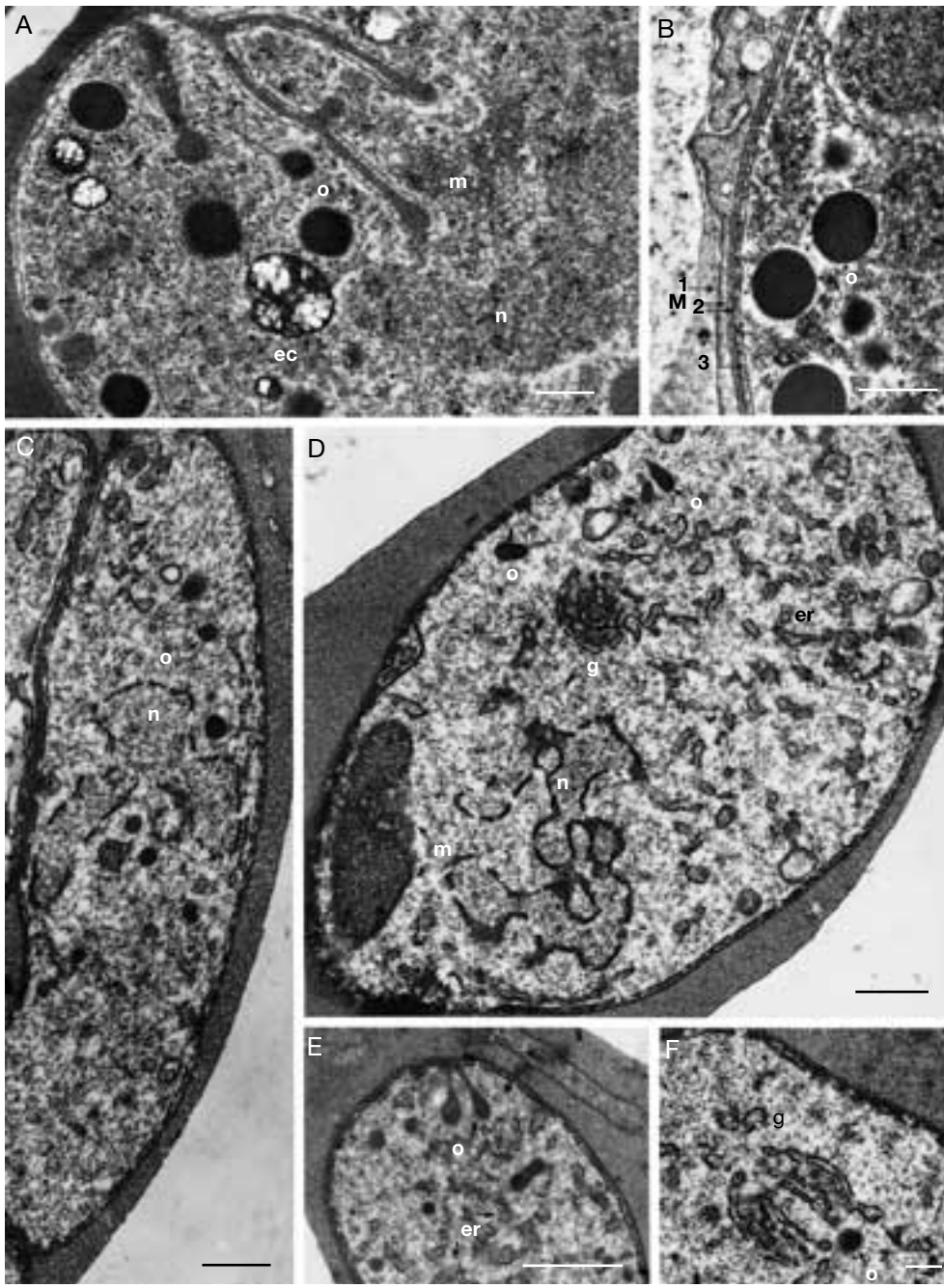

FIG. 3. — **A-B**, *H. mackerrasi* (cont.); **A**, enlarged view of intraerythrocytic *H. mackerrasi*; **B**, enlarged detail to show wall membranes of *H. mackerrasi* infecting an intrahepatic proerythrocyte; **C**-**F**; *Haemoproteus oedurae*, apparently microgametocyte stages, from *Oedura castelnaui*; **C**, general view; **D**, microgametocyte with a very large mitochondrion and a conspicuous Golgi-like organelle; **E**, anterior end, showing oblong osmiophilic bodies; **F**, detailed view of Golgi-like organelle. Abbreviations: **ec**, inclusion with crystalline deposit (hemozoin); **er**, endoplasmic reticulum and connected cisternae; **g**, Golgi; **M1**, **2** and **3**, parasites' outer, median and inner boundary membranes; **m**, mitochondrion; **n**, nucleus; **o**, osmiophilic body. Scale bars: 0.5 µm.

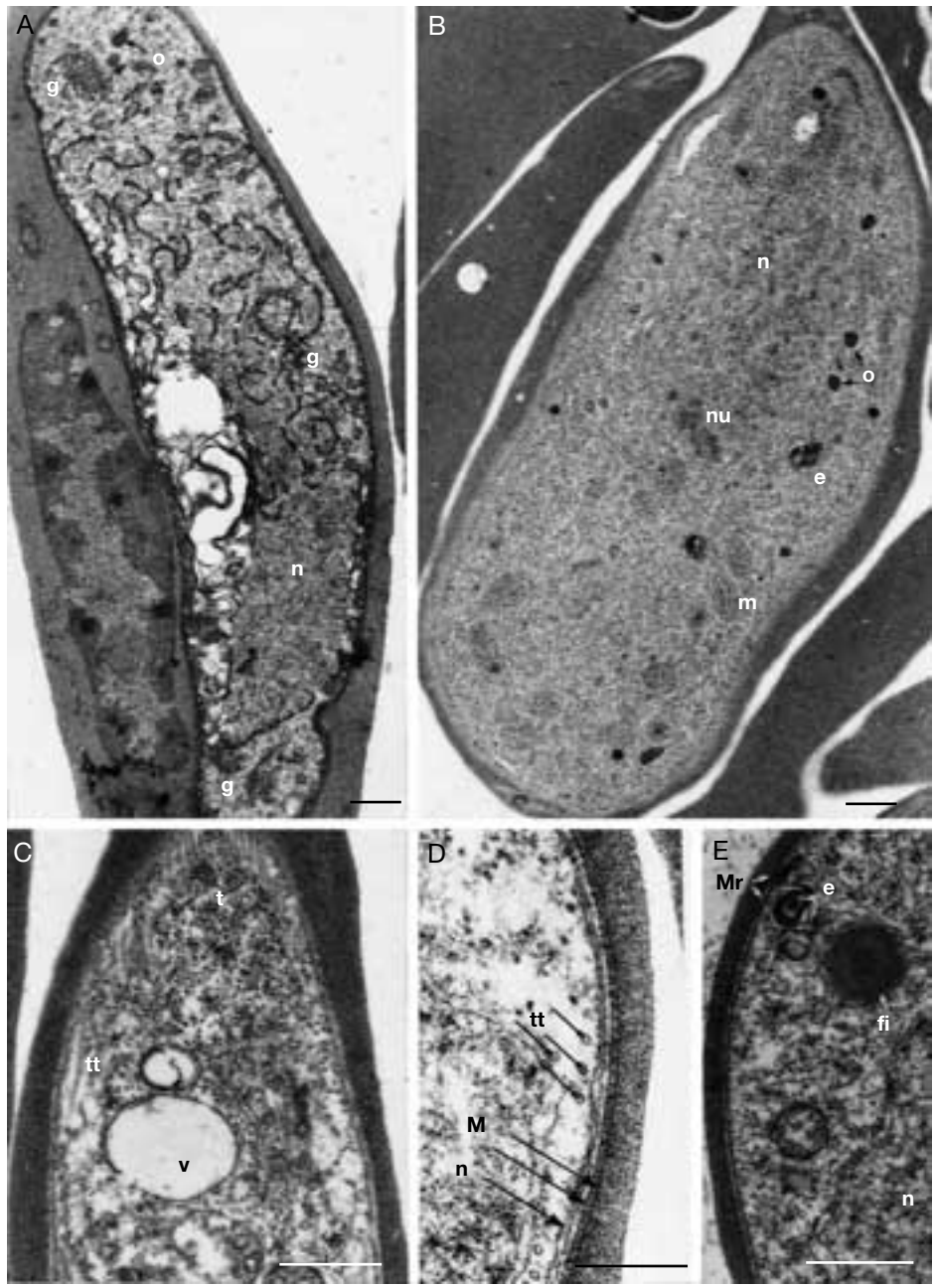

FIG. 4. — *H. oedurae* (cont.); **A**, whole view of *H. oedurae* microgametocyte with three Golgi-like organelles and a few osmiophilic bodies; **B**-**E**, *Haemoproteus ptyodactyli* from *Ptyodactylus hasselquistii*; **B**, whole view of an apparently macrogametocyte with dense ribosomal contents; note small osmiophilic bodies; **C**, juvenile gametocyte with sub-pellicular arrays of microtubules; **D**, juvenile gametocytes exhibiting wall details (M, arrows) and cross sections of sub-pellicular microtubules; **E**, gametocyte showing reforming M3 (possibly also M2) (**Mr**) and large food vacuole. Abbreviations: **e**, vacuole with phagosomal residues; **e'**, inclusion filled with electron-dense globules; **fi**, food vacuole; **g**, Golgi; **M1**, **2** and **3**, parasite's outer, median and inner boundary membranes; **m**, mitochondria; **n**, nucleus; **nu**, nucleolus; **o**, osmiophilic bodies; **t**, tubular structures; **tt**, true microtubules; **v**, vacuole. Scale bars: A-C, E, 0.5 µm; D, 0.25 µm.

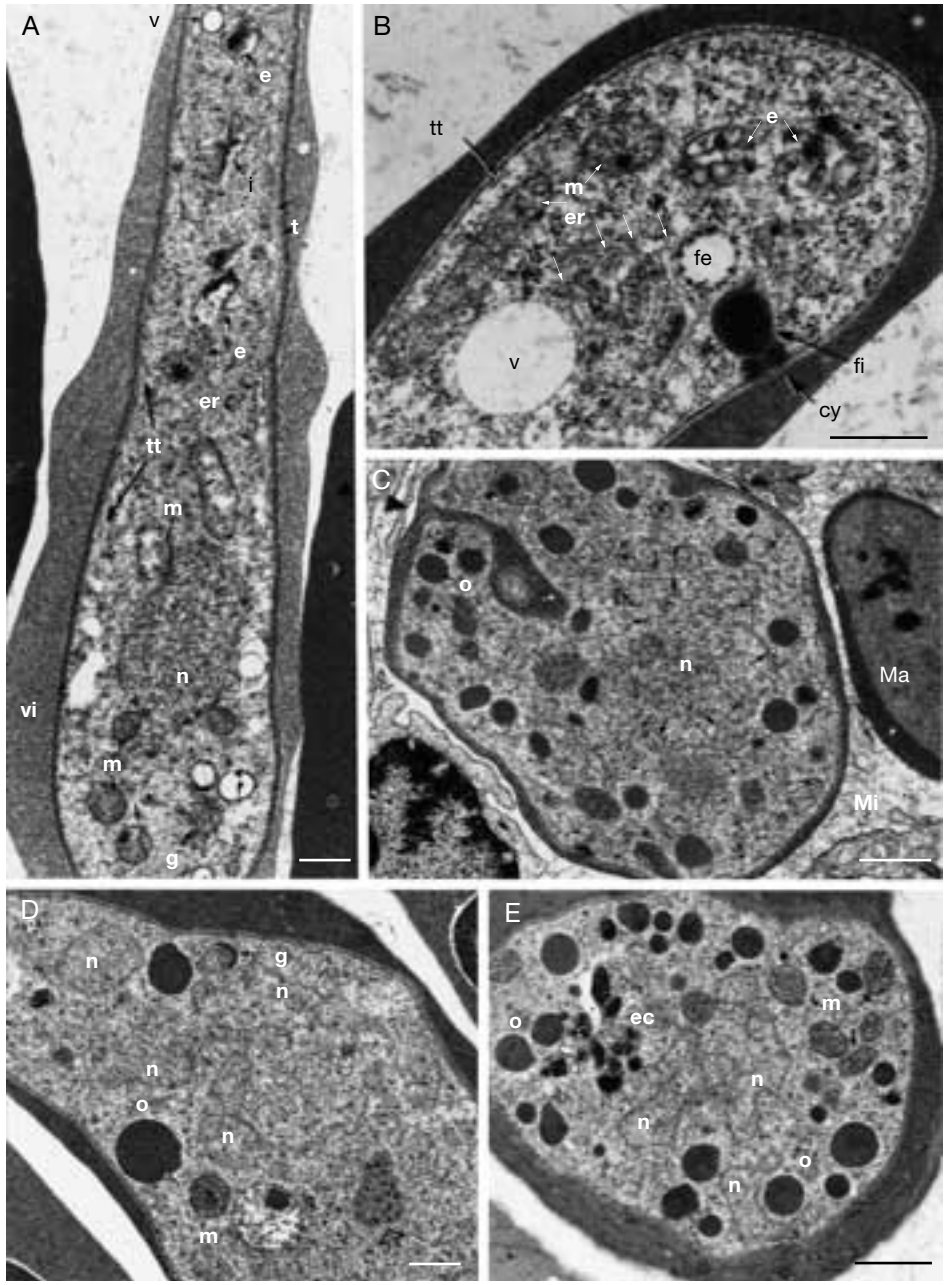

FIG. 5. — *H. ptyodactyli* (cont.); **A**, whole view of a macrogametocyte; note an inclusion of unknown entity, **i**, and sub-pellicular vacuoles, **vi**; **B**, juvenile gametocyte with conspicuous cytostome connected to food vacuole, with adjacent empty food vacuole (**fe**); **C**, folded microgametocyte (**Mi**) with lobated nucleus and numerous osmiophilic bodies, note its lower ribosomal content in comparison to the dense ribosomal content in the cytoplasm of the adjacent macrogametocyte (**Ma**); **D**, sector of a microgametocyte showing osmiophilic bodies connected by a ductule with the cell boundary zone (empty arrow - inclusion of unknown entity); **E**, cross section of a microgametocyte with numerous osmiophilic bodies. Abbreviations: **cy**, cytostome; **e**, vacuole with phagosomal residues; **ec**, inclusion with crystalline deposit (hemozoin); **er**, endoplasmic reticulum and connected cisternae; **fi**, food vacuole; **g**, Golgi; **m**, mitochondria; **n**, nucleus; **o**, osmiophilic bodies; **tt**, true microtubules; **v**, vacuole. Scale bars: A, B, D, 0.5 µm; C, 2 µm; E, 1 µm.

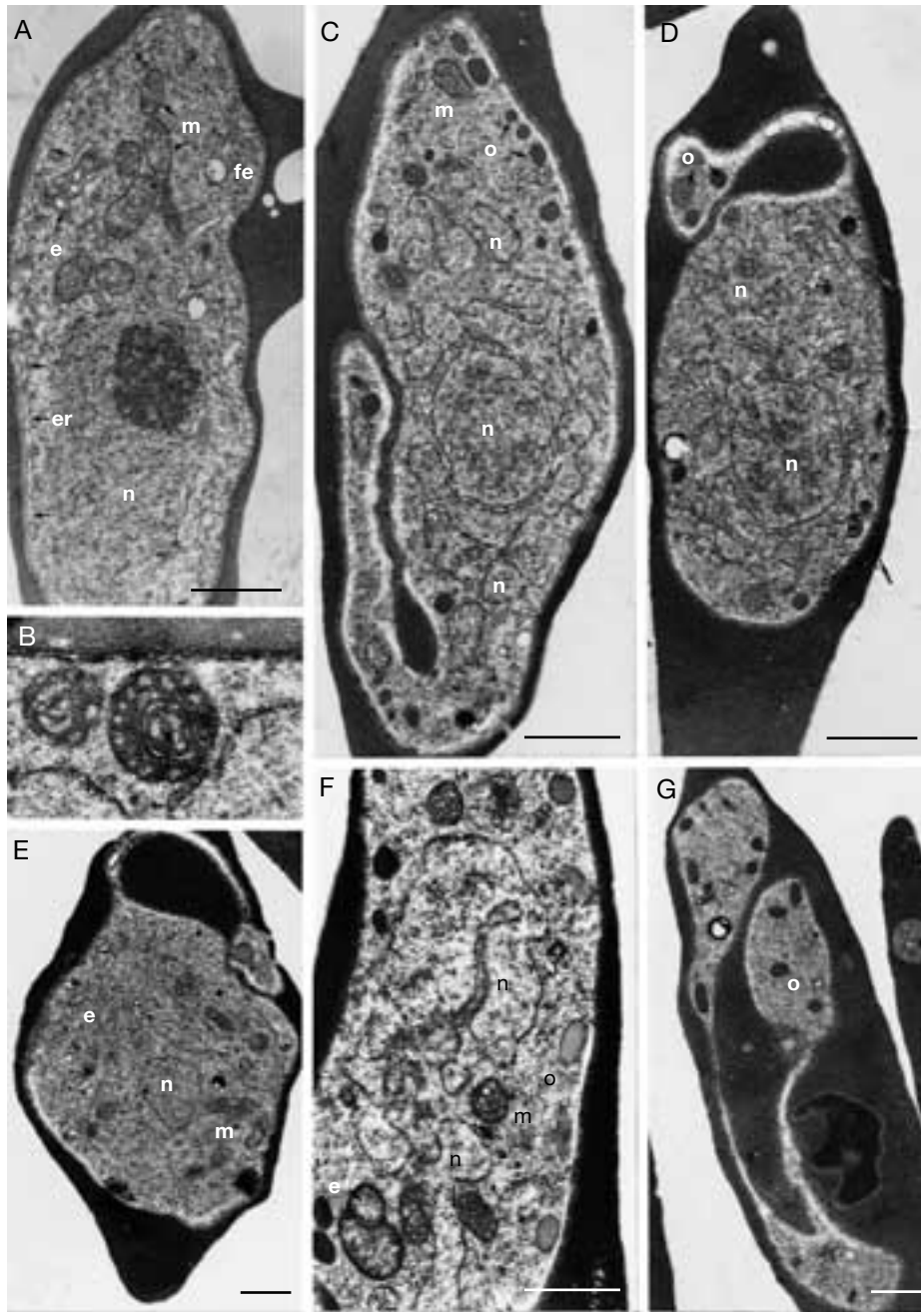

FIG. 6. — *H. ptyodactyli* (cont.); **A**, macrogametocyte with more dilute ribosomal contents and nucleus with a conspicuous nucleolus; **B**, large concentrically structured mitochondria; **C**-**G**, *Haemoproteus tarentolae* from *Tarentola mauritanica*; **C**-**D**, whole view of microgametocyte containing osmiophilic bodies, with folded attenuated ends; **E**, gametocyte with dense ribosomal contents; **F**, part of microgametocyte showing lobate nucleus, phagosomal residue inclusions and mitochondria; **G**, extremely lobate gametocyte. Abbreviations: **e**, vacuole with phagosomal residues; **er**, endoplasmic reticulum and connected cisternae; **fe**, empty food vacuole; **m**, mitochondria; **n**, nucleus; **nl**, nucleolemma; **nu**, nucleolus; **o**, osmiophilic bodies; **w**, electron-lucent space. Scale bars: A-C, E-G, 1 µm; D, 0.5 µm.

GOLGI-LIKE ORGANELLES

Single or paired clusters or aggregates of concentrically arranged tubules, vesicles or cisternae closely reminiscent of Golgi apparatuses were seen in *H. edomensis* (Figs 1B; 2D), *H. ptyodactyli* (Fig. 5A) and all *H. oedurae* studied (Fig. 3D, F). In the latter, up to three paired clusters occurred in anterior, middle and posterior positions (Fig. 4A).

MITOCHONDRIA

Mitochondria were very variable in size, with either densely packed (Figs 2A; 4B; 5C; 6C, E) or loosely spaced tubular cristae (Figs 1A, C, G; 2B; 5A, D). The internal matrix varied from dense (Fig. 2A-C, E) to lucent electron densities (Figs 2B; 6A); some contained aggregates of electron-dense substance (Fig. 5B, D). Some of the variation may have resulted from different processing conditions. A single, particularly large and condensed tubular mitochondrion was found in one *H. oedurae* (Fig. 3D). Unusual, concentrically arranged mitochondria-like organelles were observed in one *H. ptyodactyli* (Fig. 6D).

OSMIOPHILIC BODIES

Osmiophilic bodies connected by a small ductule which joined the inner pellicular membrane (Fig. 5D) occurred in variable numbers in the seeming fully differentiated gametocytes of *H. mackerrasi* (Figs 2E, F; 3A, B). Where nuclear details were discernible, osmiophilic bodies occurred in gametocytes with lobate nuclei, e.g. in microgametocytes of *H. oedurae* (Fig. 3C-F), *H. ptyodactyli* (Fig. 5C-E) and *H. tarentolae* (Figs 6B-G; 7). Small osmiophilic bodies occurred in one mature *H. ptyodactyli* macrogamont (Fig. 4B). In *H. oedurae*, the osmiophilic bodies were small and elongated (Fig. 3D); in the other species they were large and spherical.

"TRAPEZOID" ORGANELLE

An electron-dense, trapezoid body with a granular, medium-electron-dense halo bordered by electron-dense droplets was unique to gametocytes of *H. edomensis* (Figs 1C, F; 2A).

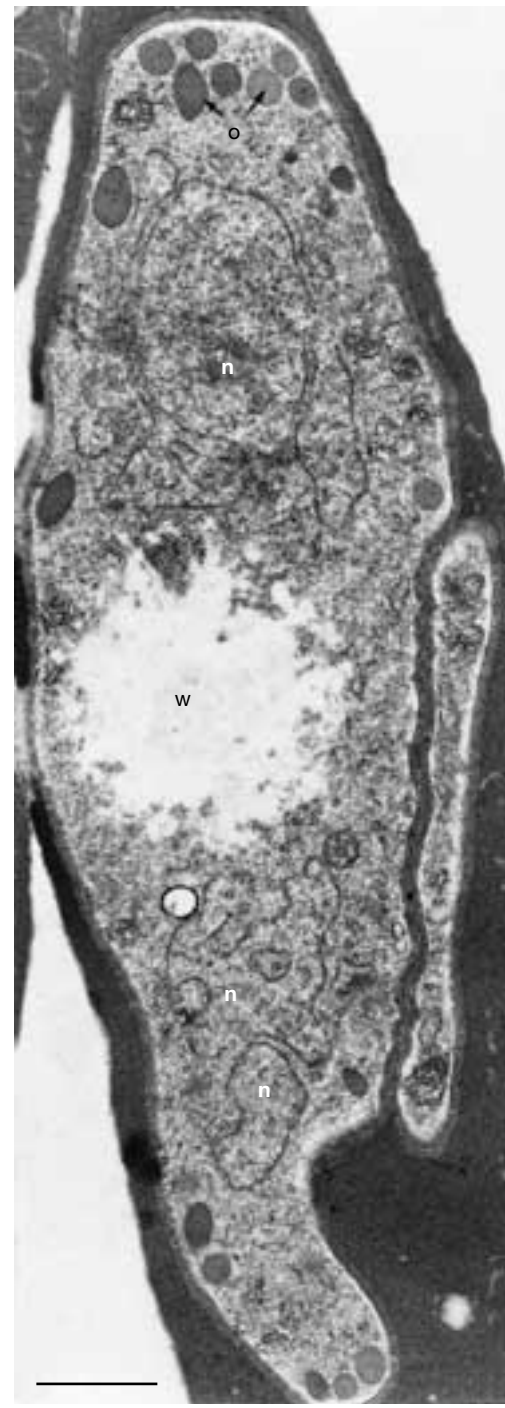

FIG. 7. — *H. tarentolae* (cont.), a microgametocyte with central, large, electron-lucent space. Abbreviations: **n**, nucleus; **o**, osmiophilic bodies; **w**, electron-lucent space. Scale bar: 1 µm.

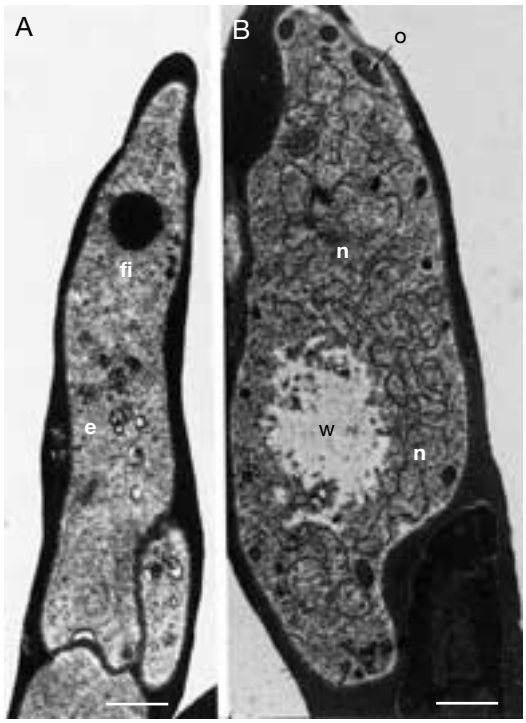

FIG. 8. — *H. tarentolae* (cont.); **A**, juvenile gametocyte; **B**, another microgametocyte with the central electron-lucent space. Abbreviations: **e**, vacuole with phagosomal residues; **fi**, food vacuole; **n**, nucleus; **o**, osmiophilic bodies; **w**, electron-lucent space. Scale bars: 1 µm.

NUCLEUS

The nucleus was either compact and oval, with one or two distinct nucleoli (as reported for macrogametocytes, Figs 1A, C, F; 4D; 6A and juvenile stages, Fig. 2B), or highly scattered into numerous lobes with no visible nucleoli (representative of that found in microgametocytes, Figs 3C, D; 4A; 5E; 6B-F; 7). In most observed specimens, both types of nuclei were enclosed by a very distinct nucleolemma (Figs 1B, C; 2D; 3C, D; 4D; 5E; 6B, C; 7), but in some, notably *H. mackerrasi,* due to fixation faults (Figs 2F; 3A), it was absent or obliterated. The nucleoplasm of both compact and scattered nuclei sometimes exhibited a higher density than the cytoplasm (notably in *H. mackerrasi*, *H. oedurae* and *H. ptyodactyli*, Figs 2F; 3A, D; 4B, D; 5A; 6A) or a very similar density (*H. edomensis* and *H. tarentolae,* Figs 1B, C, F; 2B, D; 6B, C, F; 7).

DISCUSSION

The general fine-structural organization of the presently studied species of *Haemoproteus* of lacertilian hosts conforms with that from the terrapins (Sterling 1972), the avian haemoproteids (Sterling & Aikawa 1973), and also with gametocytes of reptilian and avian *Plasmodium* spp. (Aikawa *et al.* 1969; Sterling & Aikawa 1973). At the same time, most of the presently studied saurian species also demonstrated individual characteristic, distinctive configurations. Most structurally allied were *H. edomensis* and *H. ptyodactyli*. Although all blood samples from the infected lizards were fixed and processed via the same protocol within a period of one month, processing artefacts may have contributed to the structural variations among the different species, in particular to the distinctive appearance of *H. oedurae*. The fixation environment, such as during the 5-15 s. delay in the fixation of the blood, has been shown to affect details of the observed fine structures (Bradbury & Roberts 1970). Delayed fixation also stimulates the onset of microgametocyte exflagellation (Sterling 1972; Desser 1972).

A previous light microscopic (LM) study of the same *Haemoproteus* species outlined interspecific differentiating structural and textural characters (from Giemsa stained blood films) (Paperna & Landau 1991); with only one exception in *H. tarentolae*, no correlation could be drawn, however, between LM configurations and fine-structural characters. A large electron-lucent central space seen in the *H. tarentolae* TEM images, could be seen as a poorly staining zone in many giemsa stained micro and macrogametocytes (referred to as a cisterna, Paperna & Landau 1991). Neither the stained nor the ultrastructural image provide a clue to the function of this formation.

Intraspecific variation in fine-structural configuration in addition to differences between micro- and macrogametocytes reflected differences between juvenile stages and fully differentiated, waiting, and possibly also old-senile gametocytes. The predominance of gametocytes with a rounded

TABLE 1. — List of the species studied, their hosts and fine structural affinities.

Species	Host	Locality	General configuration	Wall	Organelles	Hemozoin depots
H. edomensis	*A. stellio*	East Jerusalem (Cisjordan)	Oblong-oval, exceptionnally forming a "tail"	Characteristic of the genus, bundles of tubules	Characteristic of the genus, trapezoid, electron dense food vacuole, "golgi-like"	Vesicular/globular electron dense deposits
H. mackerrasi	*H. binoei*	Townsville (Australia)	Folded into rounded shape	Characteristic of the genus	Characteristic of the genus, many large osmiophilic bodies	Cristalline, in electron dense inclusions
H. oedurae	*O. castelnaui*	Townsville (Australia)	Oblong-oval	Characteristic of the genus microtubules	Characteristic of the genus,"golgi-like" in pairs, small and oblong osmiophilic bodies large mitochondrion endoplasmatic reticulum extensive (stressed)	Vesicular
H. ptyodactyli	*P. hasselquistii*	Jordan Valley (Cisjordan)	Oblong-oval or round folded (microgametocyte)	Characteristic of the genus, cytostome & electron dense food vacuole microtubules	Characteristic of the genus "golgi-like" (few), large vacuole, osmiophilic bodies: large (microgametocyte); few & small (macrogametocyte); "concentric mitochondria"	Globular, electron dense crystalloid (in microgametocyte)
H. tarentolae	*T. mauritanica*	Banyuls/Mer (France)	Lobated or with extending "tails"	Characteristic of the genus	Cytoplasme: central electron-lucent space, osmiophilic bodies, electron dense food vacuole	Vesicular, small, globular and crystalloid.

small nucleus in *H. edomensis* suggests them all to be macrogametocytes, while all *H. oedurae,* some *H. ptyodactyli* and most *H. tarentolae* in which gametocytes contained a scattered and lobate nucleus, appear to be microgametocytes. The finding in some species of exclusively macrogametocytes (*H. edomensis*) and in others predominantly microgametocytes (*H. oedurae*, *H. tarentolae*) confirms the observed bias in sex ratio among the different species of saurian *Haemoproteus* (Paperna & Landau 1991). Differences in nuclear configuration only partly corresponded, however, to the ex-

pected differences between macro- and microgametocytes of hemosporidians in cytoplasmic density and relative abundance of cytoplasmic organelles (Aikawa *et al*. 1969). The triple-layered pellicle is characteristic of species of both plasmodial and hemoproteid Haemosporidia of reptilian as well as avian hosts (Aikawa & Jordan 1968; Aikawa *et al*. 1969; Aikawa 1971; Sterling & Aikawa 1973): M1 has been regarded as the parasitophorous vacuole membrane, M2 the gametocyte plasmalemma and M3 the inner pellicular sac (Sinden 1983). An observed cleavage between inner and outer laminae of M1, when parasites become partly detached from the erythrocytes, suggests, that M1 is not only the parasitophorous unit membrane but is combined with an adhered component of the parasite cell wall. In the image of extracellular *H. mackerrasi* from the gut content of an engorged mosquito, the parasite's M2 was disaggregating, being reduced into undulating lamina. Both interspecific and intraspecific (due to gender and stage) variations occurred in the relative thickness of the membranes and most commonly, in the density of the intermembranal substance. M2 occurred either as a single lamina or as a true unit membrane. M3, the inner membrane, appears as two unit membranes in apposition (Aikawa & Seed 1980) some of which may be interpreted also as two membranes of an inner flat cisterna, also characteristic of the inner membranes of pellicules of Coccidia (Paperna unpubl.).

Changes in membrane properties have been noted in avian infections when drawn blood was allowed to cool for 5-15 s. before fixation (Bradbury & Roberts 1970). The relevance of ambient temperature for the heterothermic reptilian parasites is uncertain, and time to fixation was not strictly controlled in our work.

Osmiophilic bodies have been reported to be more abundant in macrogametocytes than in microgametocytes of both *H. columbae* (Bradbury & Trager 1968; Gallucci 1974) and *H. metchnikovi* (Sterling 1972), as well as in reptilian and avian *Plasmodium* spp. (Aikawa *et al.* 1969; Sterling & Aikawa 1973). Characteristic osmiophilic bodies are absent in *Parahemoproteus velans* (Desser 1972). They were completely absent from *H. edomensis* but present in the presumed macrogametocytes (the outlines of the nucleolemma were obliterated due to fixation damage) of *H. mackerrasi*. In the remaining three species, they were abundant only in the presumed microgametocytes with the scattered nucleus. One, a presumed macrogametocyte of *H. ptyodactyli,* contained very small osmiophilic bodies. In *H. oedurae* these bodies were small and elongate, reminiscent of those in mammalian plasmodia (Aikawa *et al.* 1969). The clusters of thick-walled vesicles and tubuli have been seen in both avian and reptilian *Haemoproteus* and *Plasmodium* and were referred as golgi apparatus-like by Aikawa *et al*. (1969). They seem to be the same organelles termed "dark-walled vesicles" by Galluci (1974) and "vesicular bundle" by Sterling (1972). The "trapezoid" organelle is unique, seen only in *H. edomensis,* of unknown function, and not known from other hemosporidians. This organelle might be a food vacuole at particular stage of function or homologous to an organelle termed a "lipid-like" vesicle in *H. metchnikovi* (Sterling 1972).

REFERENCES

Aikawa M. 1971. — *Plasmodium*: the fine structure of malarial parasites. *Experimental Parasitology* 30: 284-320.

Aikawa M., Huff C. G. & Sprinz H. 1969. — Comparative fine structure of the gametocytes of avian, reptilian and mammalian malarial parasites. *Journal of Ultrastructural Research* 26: 316-331.

Aikawa M. & Jordan H. B. 1968. — Fine structure of a reptilian malarial parasite. *Journal of Parasitology* 54: 1023-1033.

Aikawa M. & Seed T. M. 1980. — Morphology of Plasmodia: vol. 1, 285-340, *in* Kreier J. P. (ed.), *Malaria, Epidemiology, Chemotherapy, Morphology and Metabolism.* Academic Press, London.

Boulard Y., Landau I., Baccan D., Petit G. & Lainson R. 1987. — Observations ultrastructurales sur les formes sanguines des Garniidae (*Garnia gonatodi, G. uranoscodoni* et *Fallisia effusa*) parasites de lézards Sud-Américains. *European Journal of Protistology* 23: 66-65.

Bradbury P. C. & Roberts J. F. 1970. — Early stages in the differentiation of gametocytes of *Haemoproteus columbae* Kruse. *Journal of Protozoology* 17: 405-414.

Bradbury P. C. & Trager W. 1968. — The fine structure of mature gametes of *Haemoproteus columbae* Kruse. *Journal of Protozoology* 15: 89-102.

Desser S. S. 1972. — Gametocyte maturation, exflagellation and fertilization in *Parahemoproteus* (= *Haemoproteus*) *velans* (Coatney & Roudabush) (Haemosporidia: Haemoproteidae): an ultrastructural study. *Journal of Protozoology* 19: 287-296.

Gallucci B. B. 1974. — Fine structure of *Haemoproteus columbae* Kruse during macrogametogenesis and fertilization. *Journal of Protozoology* 21: 254-263.

Moore J. & Sinden R. 1974. — Fine structure of *Plasmodium mexicanum*. *Journal of Parasitology* 60: 825-833.

Paperna I. & Boulard Y. 1990. — Fine structure of a macrogametocyte of *Fallisia copemani* Paperna & Landau 1990 (Haemosporidia : Garnidae). *Annales de Parasitologie humaine et comparée* 65: 214-217.

Paperna I. & Landau I. 1991. — *Haemoproteus* (Haemosporidia) of lizards. *Bulletin du Muséum national d'Histoire naturelle*, 4e Série, 13 (A): 309-349.

Sinden R. E. 1983. — Sexual development of malarial parasites. *Advances in Parasitology* 22: 154-216.

Sterling C. R. 1972. — Ultrastructural study of gametocytes and gametogenesis of *Haemoproteus metchnikovi*. *Journal of Protozoology* 19: 69-76.

Sterling C. & Aikawa M. 1973. — A comparative study of gametocyte ultrastructure in avian Haemosporidia. *Journal of Protozoology* 20: 81-92.

Submitted on 12 August 1997;
accepted on 11 October 1999.